



Supporting Information

for

Get a better glimpse on sequential photoreactions of trisnorbornadienes with ^{19}F NMR spectroscopy

Julian Felix Maria Hebborn, Ben Eric Merten, Thomas Paululat and Heiko Ihmels

Beilstein J. Org. Chem. **2026**, *22*, 527–534. [doi:10.3762/bjoc.22.38](https://doi.org/10.3762/bjoc.22.38)

Experimental section and copies of spectra

Table of contents

1. Equipment.....	S2
2. Method.....	S2
3. Materials.....	S2
4. Absorption properties.....	S2
5. Photoreactions.....	S3
6. Radical-cation-induced cycloreversion.....	S3
7. Kinetic studies of the thermal back conversion.....	S3
8. STA measurement.....	S4
9. NMR spectra.....	S5
10. In situ NMR spectroscopy.....	S10
11. Kinetic simulation.....	S11
12. References.....	S12

1. Equipment

NMR spectra: JEOL ECZ 500 (^1H : 500 MHz, ^{13}C : 125 MHz, ^{19}F : 470 MHz, 25 °C), Varian VNMR-S 600 (^1H : 600 MHz, ^{13}C : 150 MHz, ^{19}F : 565 MHz, 25 °C). Reference: residual signals of CDCl_3 [$\delta(^{13}\text{C}) = 77.16$ ppm] and C_6D_6 [$\delta(^1\text{H}) = 7.16$ ppm, $\delta(^{13}\text{C}) = 128.1$ ppm], or tetramethylsilane (TMS) [$\delta(^1\text{H}) = 0.00$ ppm], or C_6F_6 [$\delta(^{19}\text{F}) = -161.6$ ppm]. Software: MestReNova. Melting points: Büchi 545 (Büchi, Flawil, CH), uncorrected. Elemental analysis: data in-house (Organic Chemistry, University of Siegen), HEKAtech EUROEA combustion analyzer. Absorption spectra: Varian Cary 100 Bio, Analytik Jena SPECORD S, in Hellma quartz glass cuvettes 115 F-QS ($d = 10$ mm); Software: Origin (OriginPro 8.5.1) with the implemented smoothing function “adjacent averaging”, factor 10. Photoreactions: 520 nm LED (Conrad electronic Nr. 181862), LUMOS 43 Atlas Photonics; 275 nm, 315 nm, 360 nm, 420 nm). In situ NMR irradiations: 405 nm LEDs [1], the ^{19}F NMR spectra are referenced relative to spectrometer calibration. Simultaneous thermal analysis (STA): STA 449C Jupiter (Netzsch), with platinum crucibles with priced lids in continuous N_2 flow.

2. Methods

Reaction mixtures were stirred with a magnetic stirring bar (400–750 rpm). Solvents were removed with a rotary evaporator at 20–40 °C under reduced pressure (360–15 mbar). Air-sensitive reactions were performed under an inert atmosphere (Ar) with Schlenk equipment. Solvents/solutions were deaerated by bubbling Argon through the solution (approx. 5 min) prior to use. Room temperature (rt) was between 20 °C and 25 °C.

3. Materials

Commercially available chemicals were purchased from BLD Pharmtech Ltd. (1,3,5-tribromo-2,4,6-trifluorobenzene), Merck KGaA [hexafluorobenzene, $\text{Ir}(\text{ppy})_3$] and Carbolution Chemicals GmbH $\text{Pd}(\text{PPh}_3)_4$, Silicycle (SiO_2 , particle size 40–63 μm). 4,4,5,5-Tetramethyl-2-(bicyclo[2.2.1]heptadien-2-yl)-1,3,2-dioxaborolane (**1e**) [2] and $\text{Ru}(\text{phen})_3(\text{PF}_6)_2$ [3] were prepared according to literature. *n*-Hexane was purified by distillation prior to use.

4. Absorption properties

Solutions ($c = 20$ μM , $V = 3.00$ mL) of the norbornadiene **1f** in MeCN, cyclohexane, MeOH, EtOAc, THF, CH_2Cl_2 , CHCl_3 , and benzene were prepared by the evaporation of a stock solution of **1f** in MeCN ($c = 1$ mM, $V = 60$ μL) under a nitrogen stream followed by the addition of the corresponding solvent. The absorption spectra were subsequently measured (20 °C).

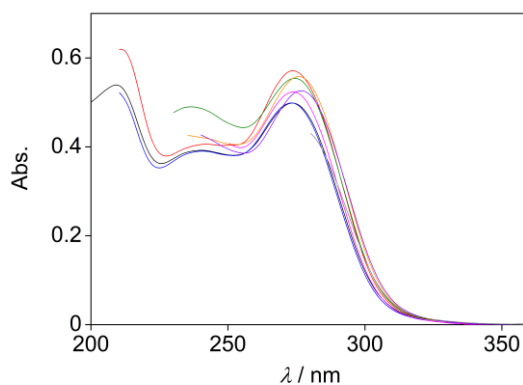


Figure S1: Absorption spectra of **1f** ($c = 20$ μM) in MeCN (—), cyclohexane (—), MeOH (—), EtOAc (—), THF (—), CH_2Cl_2 (—), CHCl_3 (—) and benzene (—).

5. Photoreactions

Photometric investigation of the cycloaddition and cycloreversion reaction

The cycloaddition reaction was investigated photometrically by the direct irradiation ($\lambda = 315$ nm) of **1f** in MeCN ($c = 20$ μ M, $V = 3.00$ mL). The irradiation was stopped, when only negligible change in absorption occurred.

NMR-Spectroscopic investigation of the cycloaddition and cycloreversion reaction

A solution of **1f** ($c = 6$ mM, C_6D_6) was irradiated with LUMOS 43 ($\lambda = 315$ nm), and the product mixture was analyzed with 1H NMR spectroscopy (Figure S11).

The photocatalyzed isomerization of **1f** ($c = 15$ mM, C_6D_6) in the presence of $Ir(ppy)_3$ (10 mol %) or the flavin **4** (10 mol %) was followed by in-situ 1H and ^{19}F NMR spectroscopy ($\lambda = 405$ nm, 8.0 mW or 2.1 mW optical energy).

6. Radical-cation-induced cycloreversion

Magic blue (0.15 mg, 7 mol %) was added to a solution of the quadricyclane **2f^{0,3}** ($c = 2$ mM, $CDCl_3$). The subsequently recorded 1H NMR spectrum showed complete conversion to the norbornadiene **1f** (Figure S12).

7. Kinetic studies of the thermal back conversion

The thermally induced cycloreversion of **2f^{0,3}** was monitored by absorption spectroscopy (Figure S2). A solution of the norbornadiene ($c = 20$ μ M, $V = 3$ mL, isooctane) was irradiated for 3.5 h with $\lambda_{ex} = 315$ nm to give the corresponding solution of the quadricyclane **2f^{0,3}**. The increasing absorption ($\lambda_{abs.} = 274$ nm) of the formed norbornadiene was determined at 70 °C, 80 °C, and 90 °C.

Considering that the cycloreversion is a monomolecular reaction, first-order reaction kinetics were applied for further analysis (Eq. 1).

$$-\frac{d[QC]}{dt} = \frac{d[NBD]}{dt} = k \Leftrightarrow [NBD]_t = [NBD]_{t=0} e^{-kt} \quad (\text{Eq. 1})$$

In equation 1, [QC] is the concentration of the quadricyclane **2f^{0,3}**, [NBD] is the concentration of the norbornadiene **1f** and t is the time. The constant k describes the rate constant of the cycloreversion at a certain temperature and was obtained by an exponential fit.

With the rate constants k at their distinct temperature, $\ln(k/T)$ was plotted versus $1/T$ in an Eyring plot. The activation enthalpy ΔH was determined from the slope, while the entropy ΔS was determined from the y-intercept. The rate constant k for $T = 25$ °C was determined according to Eq 3.

$$\ln\left(\frac{k}{T}\right) = \frac{-\Delta H^\ddagger}{R} \frac{1}{T} + \ln\left(\frac{k_B}{h}\right) + \frac{\Delta S^\ddagger}{R} \quad (\text{Eq. 2})$$

$$k = \frac{k_B T}{h} e^{-\frac{\Delta H^\ddagger - T\Delta S^\ddagger}{RT}} \quad (\text{Eq. 3})$$

In equations 2 and 3, k_B is the Boltzmann constant, T is the temperature, h is the Planck constant and R is the gas constant.

With the temperature-adjusted rate constant k , the half-life of the quadricyclane $2\mathbf{f}^{0,3}$ was determined (Eq. 4).

$$t_{1/2} = \frac{\ln(2)}{k} \quad (\text{Eq. 4})$$

In equation 4, $t_{1/2}$ is the half-life and k is the rate constant of the cycloreversion at $T = 25\text{ }^\circ\text{C}$.

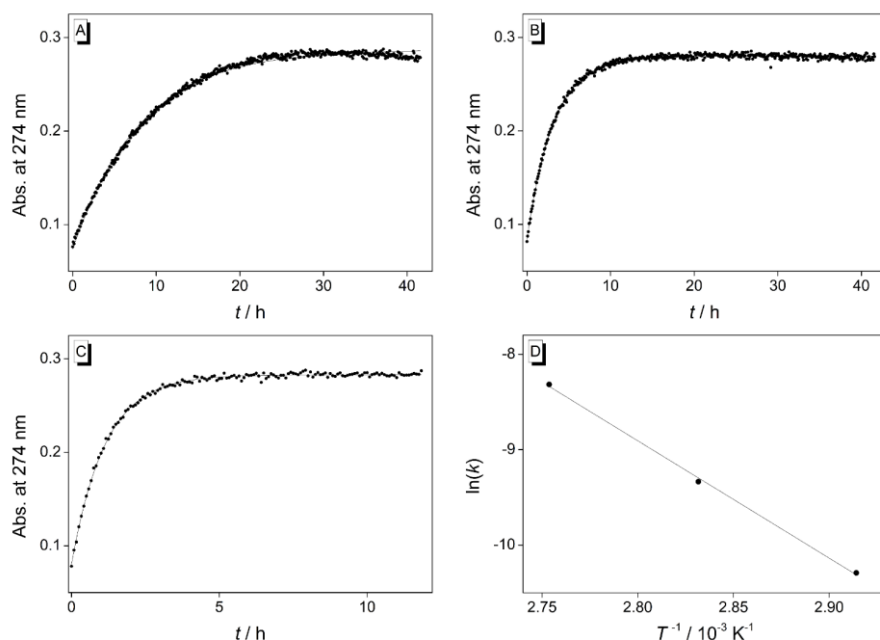


Figure S2: Photometric analysis of the thermal back reaction of $2\mathbf{f}^{0,3}$ ($c = 20\ \mu\text{M}$, $V = 3\ \text{mL}$) in isooctane at $70\text{ }^\circ\text{C}$ (A), $80\text{ }^\circ\text{C}$ (B), and $90\text{ }^\circ\text{C}$ (C). The line represents the fit of the exponential function (A–C). The straight line represents the fit in the Eyring plot (D).

8. STA measurement

The quadricyclane $2\mathbf{f}^{0,3}$ (8.03 mg) was sealed in a platinum crucible with a pierced lid and placed in the calorimeter at room temperature under a nitrogen-gas atmosphere. The following temperature program was used to measure the heat release [4].

1. Maintain $25\text{ }^\circ\text{C}$ for 15 min.
2. Heat from $25\text{ }^\circ\text{C}$ to $250\text{ }^\circ\text{C}$ with $5.0\text{ }^\circ\text{C min}^{-1}$.
3. Cool to $70\text{ }^\circ\text{C}$ with $5.0\text{ }^\circ\text{C min}^{-1}$.
4. Heat from $70\text{ }^\circ\text{C}$ to $250\text{ }^\circ\text{C}$ with $5.0\text{ }^\circ\text{C min}^{-1}$.
5. Cool to $25\text{ }^\circ\text{C}$ with $5.0\text{ }^\circ\text{C min}^{-1}$.

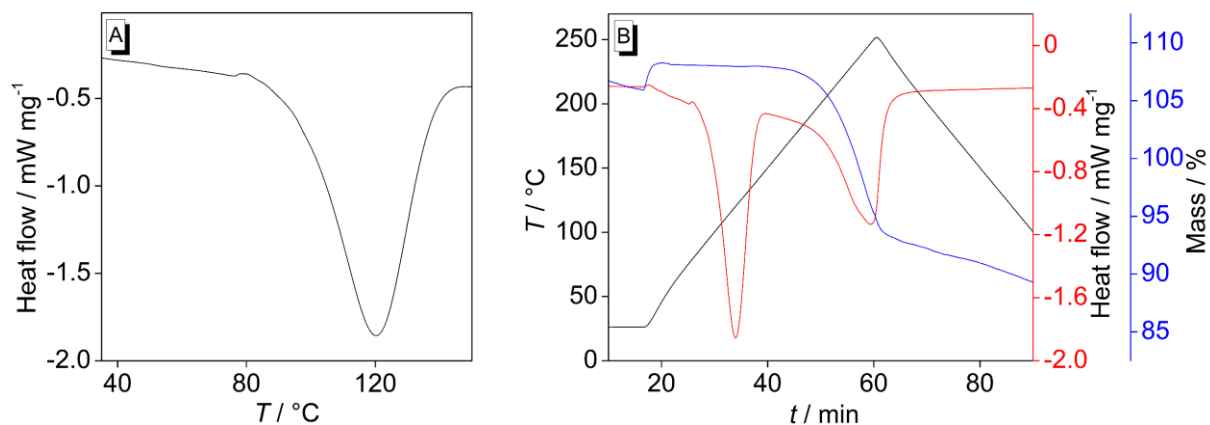


Figure S3: Extracted thermogram (A) from the STA measurement (B) of the quadricyclane $2\mathbf{f}^{0.3}$. Negative signals of the heat flow represent exothermic processes, while positive signals represent endothermic processes (A, B). In the STA measurement (B) the heating rate (\blackrightarrow), heat flow ($\color{red}\blackrightarrow$), and mass ($\color{blue}\blackrightarrow$) are represented.

9. NMR spectra

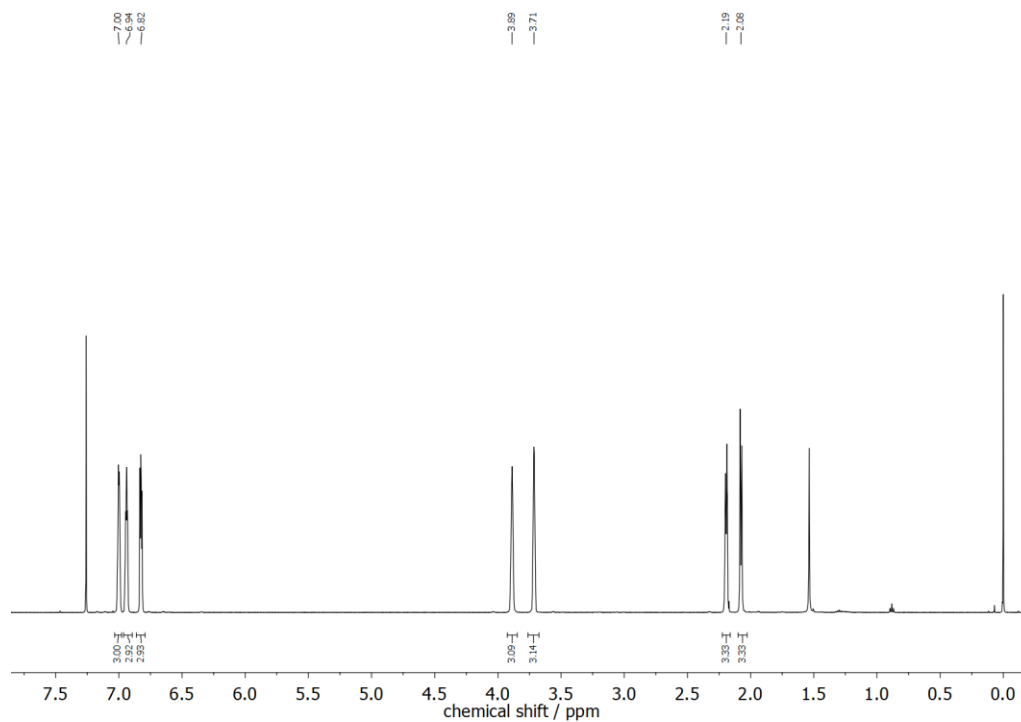


Figure S4: ^1H NMR spectrum (500 MHz) of $1\mathbf{f}$ in CDCl_3 .

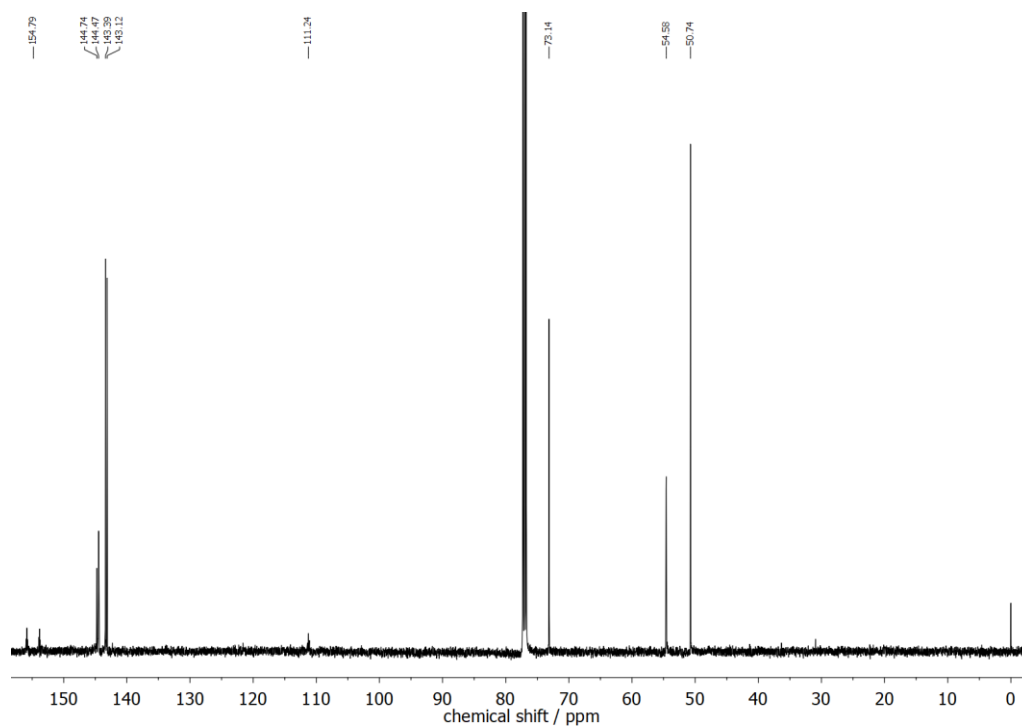


Figure S5: ^{13}C NMR spectrum (125 MHz) of **1f** in CDCl_3 .

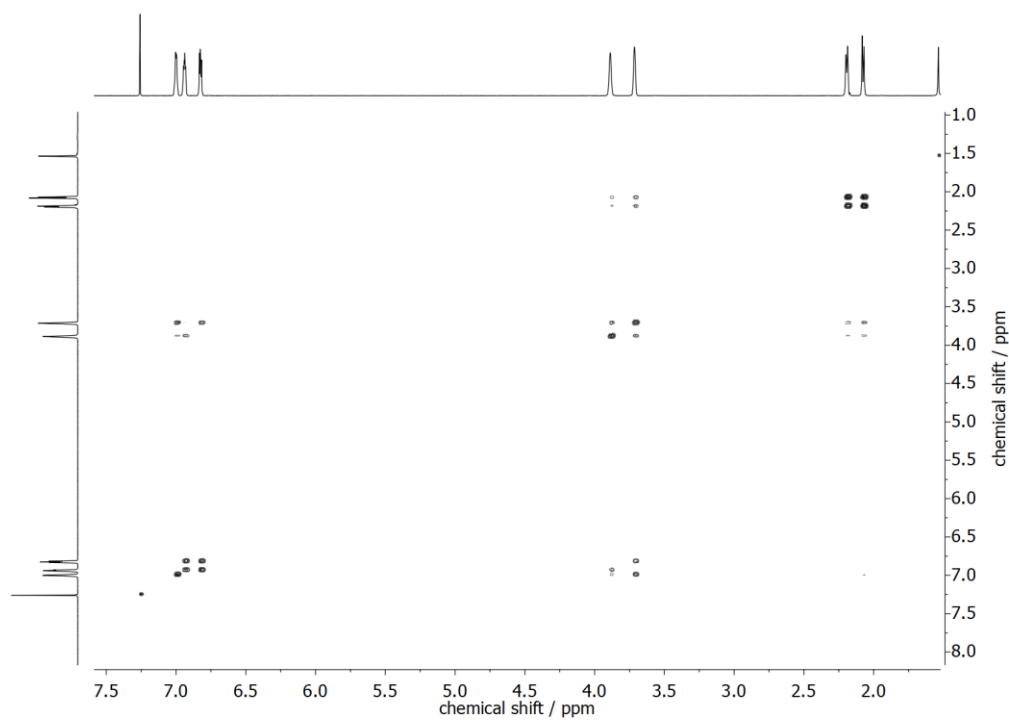


Figure S6: $^1\text{H},^1\text{H}$ -COSY NMR spectrum (500 MHz) of **1f** in CDCl_3 .

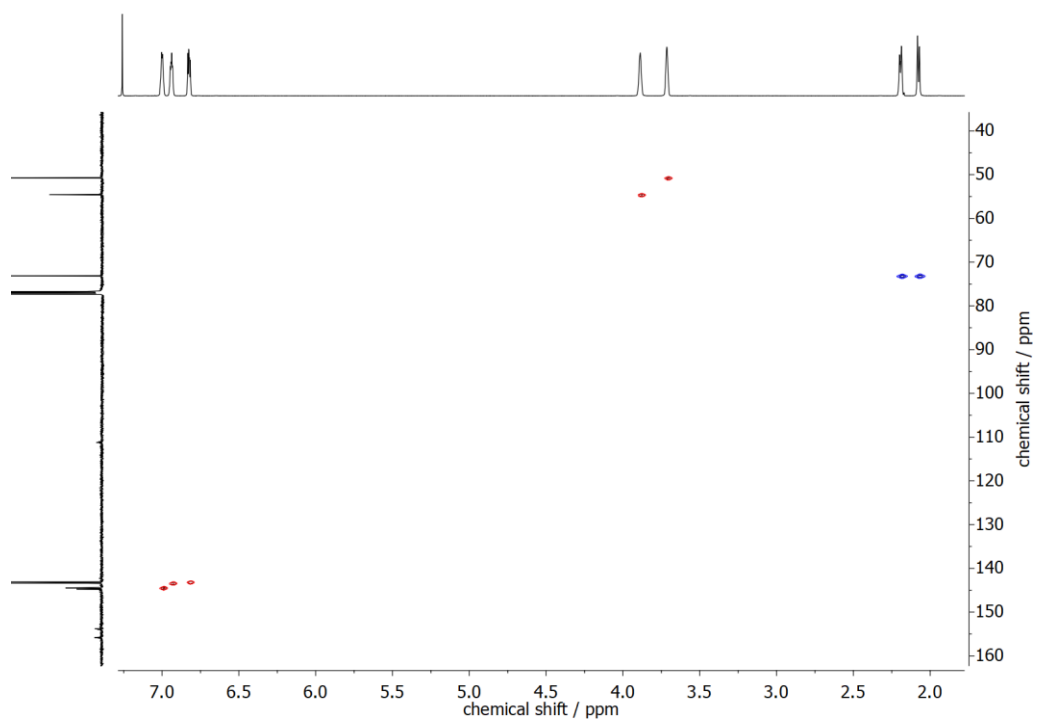


Figure S7: HSQC NMR spectrum (500 MHz) **1f** in CDCl₃.

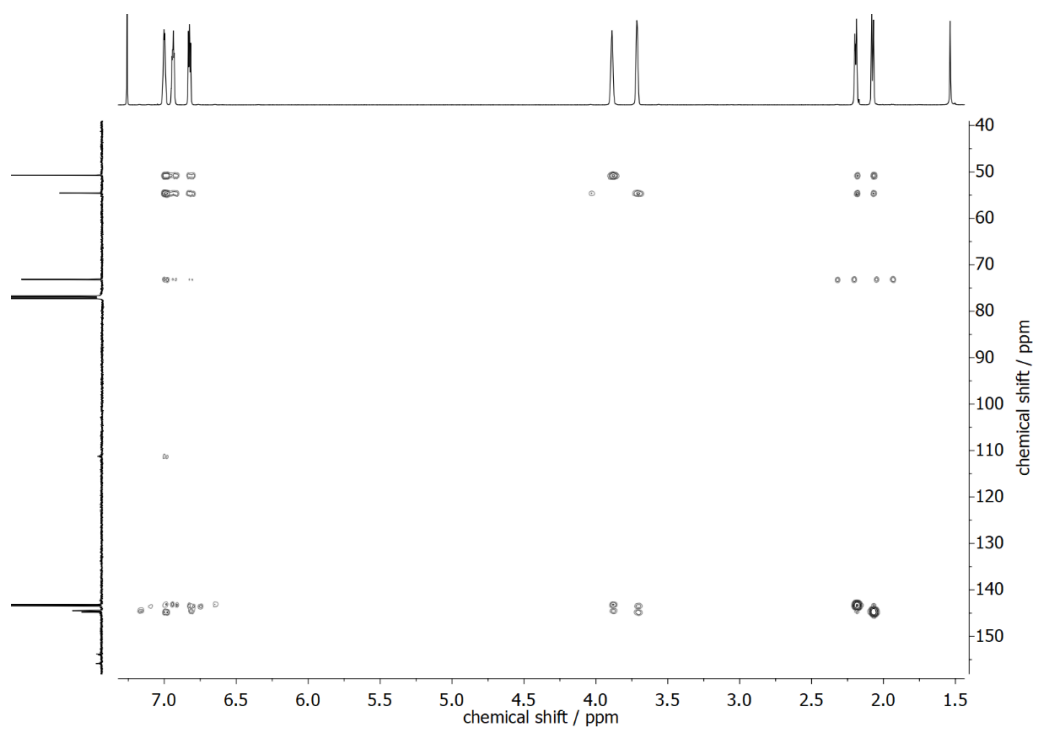


Figure S8: HMBC NMR spectrum (500 MHz) of **1f** in CDCl₃.

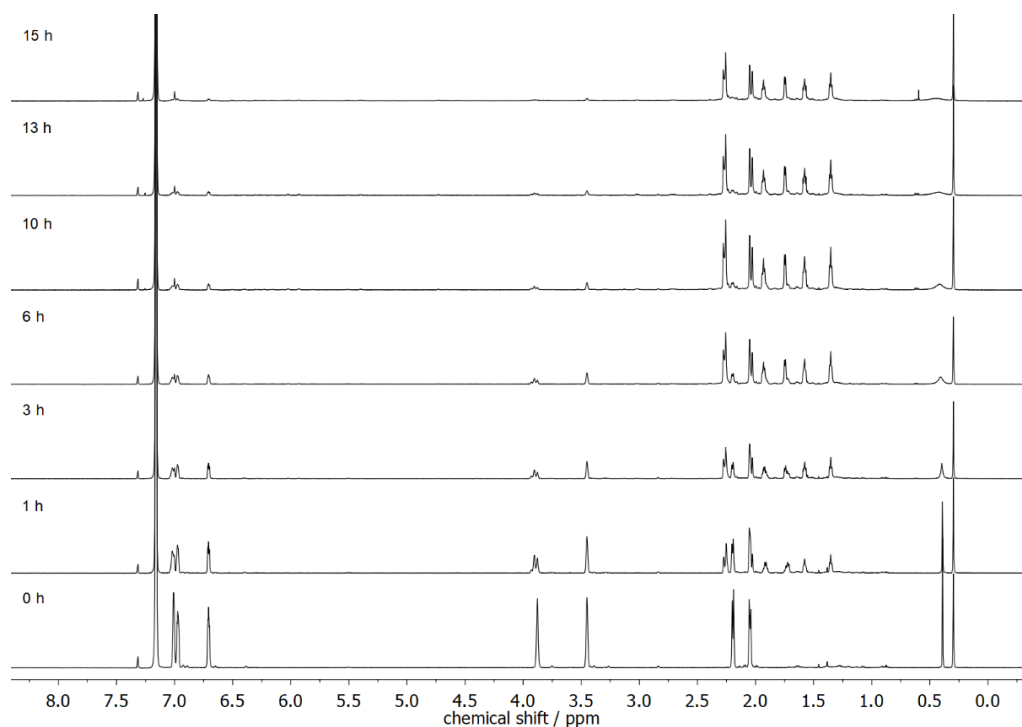


Figure S11: Determination of the photostationary state (PSS) by monitoring the cycloaddition reaction of **1f** ($c = 6 \text{ mM}$) in C_6D_6 upon irradiation with LUMOS 43 ($\lambda_{\text{ex}} = 315 \text{ nm}$) with ^1H NMR spectroscopy (500 MHz).

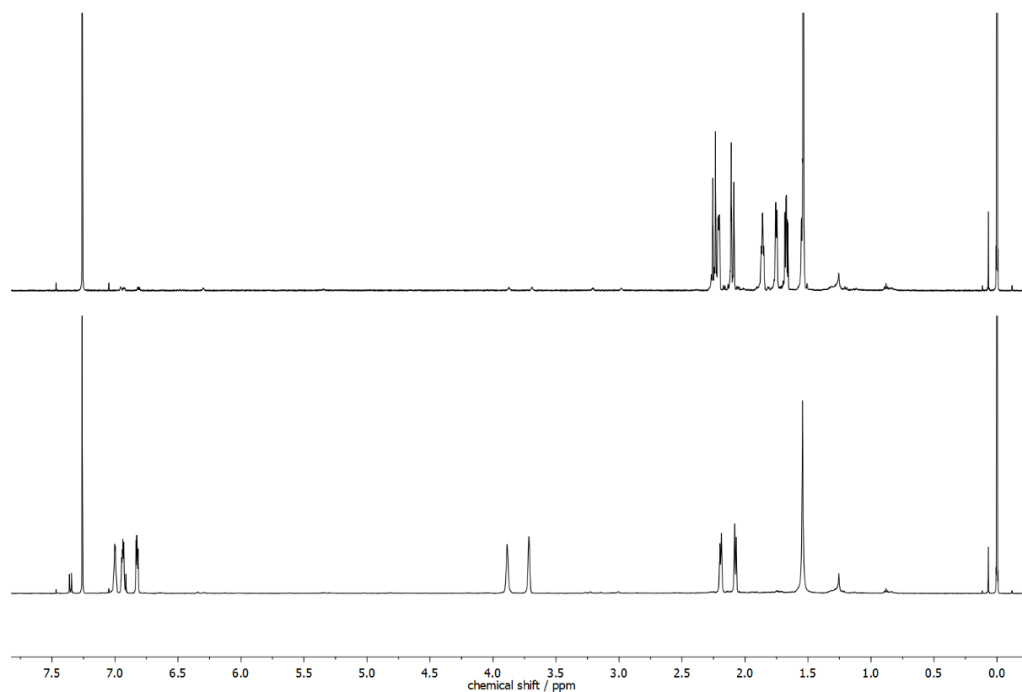


Figure S12: ^1H NMR spectra (500 MHz) of **2f^{0.3}** ($c = 2 \text{ mM}$, CDCl_3 , top spectrum) and after addition of magic blue (7.5 mol %, bottom spectrum)

10. In situ NMR spectroscopy

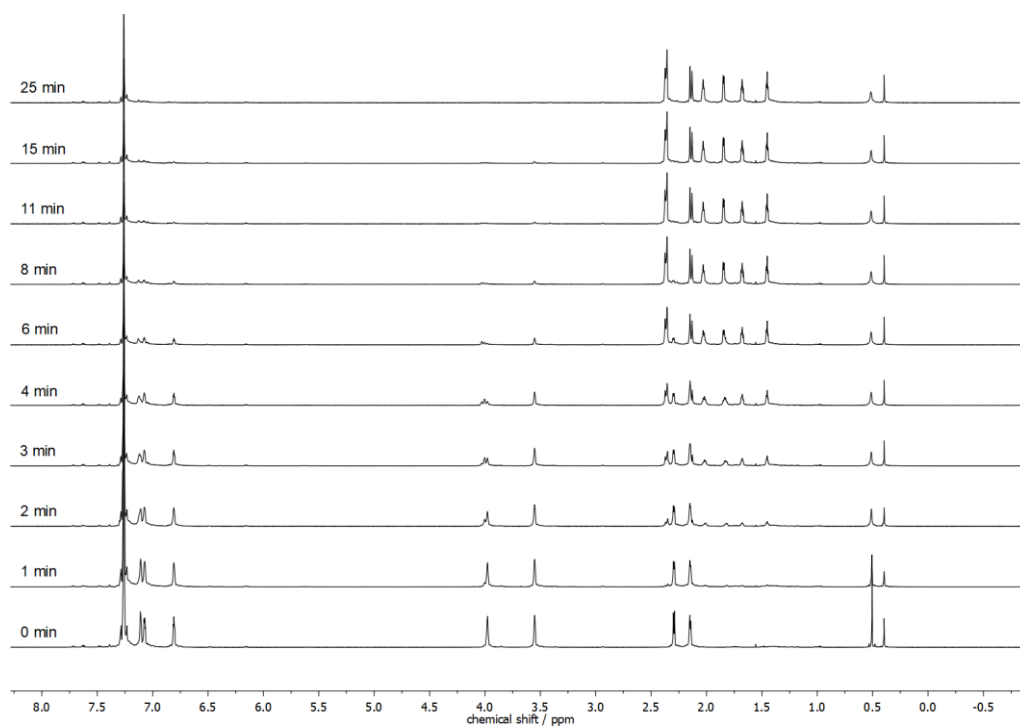


Figure S13: In situ ^1H NMR-spectroscopic analysis (600 MHz) of the photoreaction of **1f** (15 mM) in the presence of $\text{Ir}(\text{ppy})_3$ (10 mol %) in C_6D_6 at different irradiation times ($\lambda_{\text{ex}} = 405$ nm, 8.0 mW). Spectra were recorded in intervals of 1 min, only selected spectra are shown.

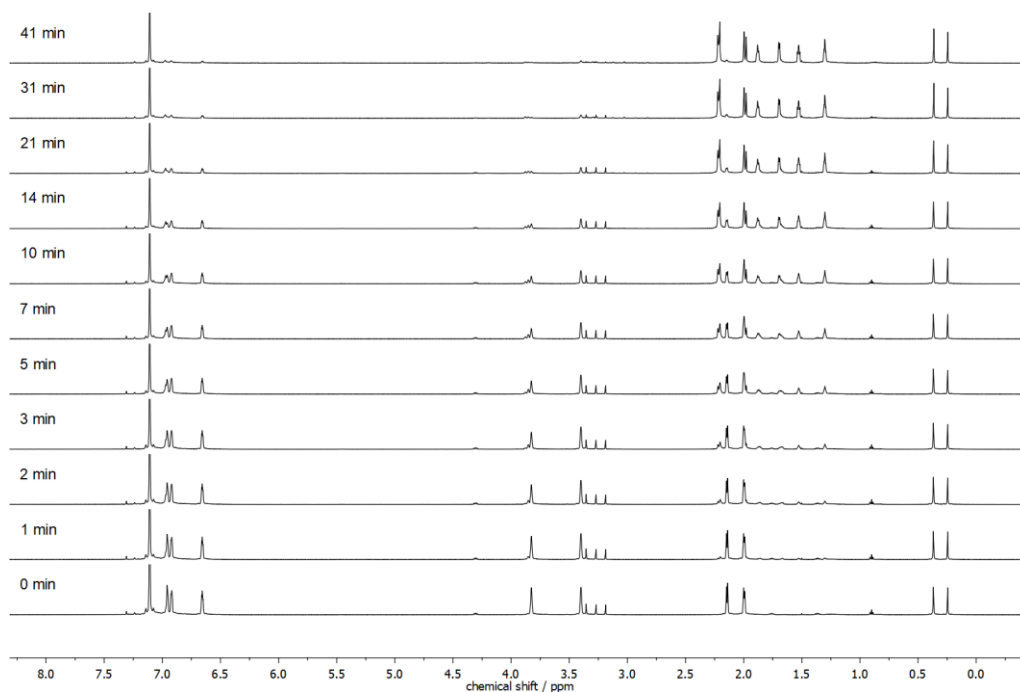


Figure S14: In situ ^1H NMR-spectroscopic analysis (600 MHz) of the photoreaction of **1f** (15 mM) in the presence of flavine **4** (10 mol %) in C_6D_6 at different irradiation times ($\lambda_{\text{ex}} = 405$ nm, 2.1 mW). Spectra were recorded in intervals of 1 min, only selected spectra are shown.

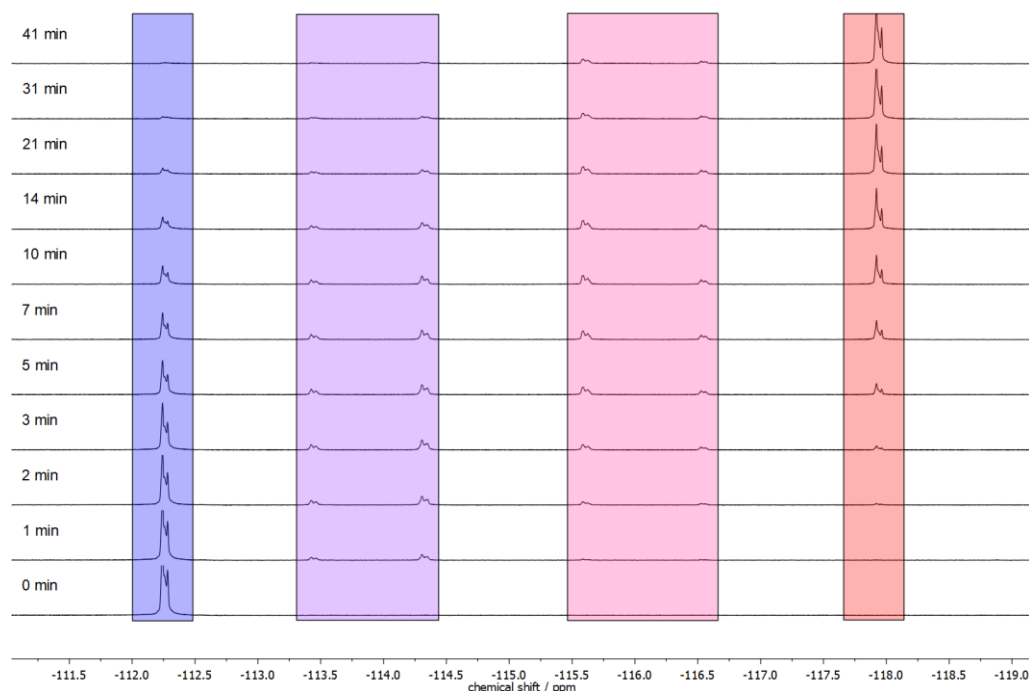


Figure S15: In situ ^{19}F NMR spectroscopic analysis (565 MHz) of the photoreaction of **1f** (15 mM) in the presence of flavine (**4**) (10 mol %) in C_6D_6 at different irradiation times ($\lambda_{\text{ex}} = 405 \text{ nm}$, 2.1 mW). The blue band indicates the signals of **1f**, the purple band indicates the signals of **2f^{2,1}**, the pink band indicates the signals of **2f^{1,2}**, and the red band indicates the signals of **2f^{0,3}**. Spectra were recorded in intervals of 1 min, only selected spectra are shown.

11. Kinetic simulation

The rate constants (k_1 , k_2 , k_3) of the photosensitized cycloaddition reaction of **1f** were estimated by fitting the change of concentrations of the starting material **1f**, photoproducts **2f^{2,1}**, **2f^{1,2}**, and **2f^{0,3}** and photocatalyst **4** during reaction time. For this purpose, the Complex Pathway Simulator COPASI [5] was used in combination with the Levenberg–Marquardt algorithm. The concentrations were obtained by integration of the ^1H and ^{19}F signals as examined by in situ NMR-spectroscopic analysis (Figure S14 and S15).

It was assumed that the reaction is a stepwise and irreversible process (Eq. 5, 6, 7). The ground state and excited state of the photocatalyst were not explicitly considered, but rather treated as a collision factor. Hence, three reactions were used for the analysis (Eq.5–7).



In equation 5, 6, 7, k_1 , k_2 , and k_3 represent the respective rate constants of these reactions.

Over the course of the reaction photobleaching occurred (Figure S14) and was considered in the fitting according to (Eq. 8).

$$\lim_{t \rightarrow \infty} [\mathbf{4}]t \xrightarrow{k_{\text{bleach}}} 0 \quad (\text{Eq. 8})$$

In equation 8, $[\mathbf{4}]$ is the concentration of the photocatalyst, t is the time and k_{bleach} the rate constant of the bleaching process.

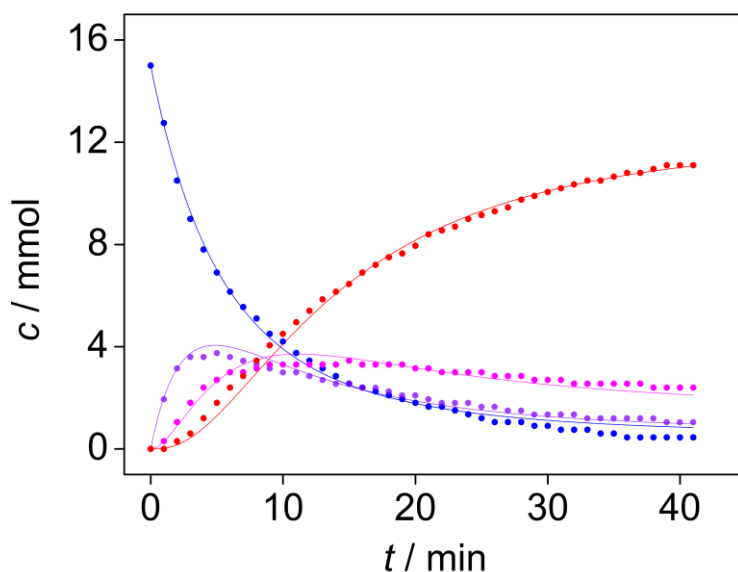


Figure S16: Plot of the concentration of components in the reaction mixture versus reaction time of **1f** in the presence of **4** ($\lambda_{\text{ex}} = 405 \text{ nm}$); blue: **1f**; purple: **2f^{2,1}**; pink: **2f^{1,2}**; red: **2f^{0,3}**. The solid lines represent the corresponding fit of the experimental data to the kinetic model.

Table S1: Rate constants k_1 , k_2 , and k_3 of the stepwise photoreaction of trisnorbornadiene **1f**.

	$k / \text{L mmol}^{-1} \text{min}^{-1}$ ^a	SD / $10^{-3} \text{L mmol}^{-1} \text{min}^{-1}$
k_1	0.12	1.0
k_2	0.20	2.6
k_3	0.17	2.2

^a Rate constant obtained from fit of experimental data to kinetic model (eq. 5–7).

^b Standard deviation from parameter estimation.

12. References

1. Paululat, T.; Rabe, M.; Berdnikova, D. V. *J. Magn. Reson.*, **2021**, *327*, 106990.
2. Schulte, R.; Ihmels, H. *Beilstein J. Org. Chem.*, **2022**, *18*, 368–373.
3. Wang, W.; Zhang, J.; Wang, H.; Chen, L.; Bian, Z. *Appl. Catal. Gen.*, **2016**, *520*, 1–6.
4. Schulte, R.; Afflerbach, S.; Paululat, T.; Ihmels, H. *Angew. Chem. Int. Ed.*, **2023**, *62*, e202309544.
5. Hoops, S.; Sahle, S.; Gauges, R.; Lee, C.; Pahle, J.; Simus, N.; Singhal, M.; Xu, L.; Mendes, P.; Kummer, U. *Bioinformatics*, **2006**, *22*, 3067–3074.